ASSESSMENT OF HIGHER-ORDER EXPONENTIAL OPERATORS FOR THE SIMULATION OF HIGH-CAPACITY OPTICAL COMMUNICATION SYSTEMS BY THE SPLIT-STEP FOURIER METHOD

P. B. Harboe[1] and J. R. Souza[2]

[1]*Telecommunication Engineering Department, Federal Fluminense University, Rua Passo da Pátria, 156, Niterói – RJ, CEP 24210-240, Brazil; Fax: + 55 21 6203935; E.mail: paula@telecom.uff.br*

[2]*Center for Telecommunication Studies, Pontifical Catholic University of Rio de Janeiro, Rua Marquês de São Vicente, 225, Rio de Janeiro – RJ, CEP 22451-041, Brazil; Fax: + 55 21 31141154; E.mail: jrsouza@cetuc.puc-rio.br*

Abstract

The use of higher-order exponential operators in conjunction with the Split-Step Fourier (SSF) method is explored for the numerical solution of the generalised nonlinear Schrödinger equation, which describes pulse propagation in dispersive, nonlinear optical fibers. It is shown that although the higher-order operators afford a reduction in the discretization error, the total error increases with the order of the operator, a fact that is attributed to the corresponding increase in the number of fast Fourier transforms (FFTs) required by the SSF method.

Key words: Nonlinear fiber optics, optical solitons, symplectic integrators.

1. Introduction

The propagation of pulses in optical fibers is described by the generalised nonlinear Schrödinger equation (GNLSE) [1], which takes into account the fiber losses, nonlinear effects, and higher-order chromatic dispersion. The GNLSE is a partial differential equation, whose order depends on the nonlinear and dispersion effects considered. As this equation is not amenable to analytical solution, the use of numerical integration techniques is mandatory. Different schemes were proposed for the numerical integration of the nonlinear Schrödinger equation [2]-[4], of which the Split-Step Fourier Method (SSF) gained preference due to its superior performance in comparison with other methods, such as the finite difference methods, as demonstrated in [3], and the Fourier series method [4]. The SSF method introduces two sources of errors: the non-commutative nature of the exponential operators required to separate the linear and nonlinear parts of the GNLSE, which are independently

 ISSN 1516-7399

solved in the frequency and time domains, respectively, and the fast Fourier transform (FFT) used to link the two domains. In practice, the former leads to a spatial discretization error, as the magnitude of the error is related to the step size of the numerical integration.

This paper assesses the performance of exponential operators of first-, second-, and fourth-orders. It is shown that the higher-order exponential operators allow for smaller spatial discretization errors, but lead to a considerable increase of the total error, which is attributed to the greater number of FFTs required by the SSF method. Through the simulation of several examples, considering both single and multiple channel signals, it is shown that the first-order operator yields results of the same quality as those obtained with the second-order one, which is universally used in conjunction with the SSF method. The simulations show clearly that the dominant source of error in the SSF method is associated with the FFT, a fact that does not seem to have been considered before.

The paper is organized as follows: the next section introduces the basic formulation for the propagation of pulses in optical fibers, considering both single and multiple channel signals, and a brief description of the Split-Step Fourier Method is given. Then, in Section 3 numerous simulations concerning single and multiple channel optical communication systems are reported, and the main results are presented. Finally, conclusions are drawn in Section 4.

2. Formulation

Only monomode optical fibers are considered here, as these are the ones of interest for long distance, high-capacity optical communication systems. A brief description of the Split-Step Fourier Method is presented, considering both single and multiple channel signals.

2.1 Single Channel Signals

Under the slowly varying envelope approximation, the complex amplitude of the electric field in a monomode optical fiber is described by the generalised nonlinear Schrödinger equation (GNLSE) [1]:

$$\frac{\partial A}{\partial z} = -\frac{j}{2}\beta_2 \frac{\partial^2 A}{\partial T^2} + \frac{1}{6}\beta_3 \frac{\partial^3 A}{\partial T^3} - \frac{\alpha}{2} A + j\gamma |A|^2 A \qquad (1)$$

where A = A(z,T) is the complex amplitude of the electric field, z is the distance along the fiber length, and T is the time measured in a referential frame moving at the group velocity v_g ($T = t - z/v_g$; t is the absolute time). β_2 e β_3 are the second- and third-order dispersion parameters, respectively; α is the linear loss coefficient, and γ describes the nonlinear effects [1].

Only the basic principles of the Split-Step Fourier method will be presented here, as detailed descriptions can be found elsewhere [1]-[3]. Initially, the equation (1) is re-written as:

$$\frac{\partial A}{\partial z} = [L + N(z)] \cdot A \qquad (2)$$

 ISSN 1516-7399

where L is a linear differential operator, which takes into account all the dispersion effects; N is a nonlinear operator, which accounts for the losses and nonlinear effects of the optical fiber. The L and N operators are conveniently and separately evaluated in the frequency and time domains, respectively. The two domains are linked through the fast Fourier transform.

In reality, dispersion and nonlinearities act simultaneously along the length of the optical fiber. An approximate representation is given by the Split-Step Fourier Method, assuming that dispersion and nonlinearities act independently over a very short distance Δz along the fiber. Formally, the solution of the equation (2) is advanced on step Δz along the fiber as:

$$A(z+\Delta z,T)=\exp\left\{\int_{z}^{z+\Delta z}[L+N(z)]dz'\right\}\cdot A(z,T) \tag{3}$$

The SSF method maskes use of exponential operators to approximate the right-hand side of the equation (3). The simplest and lowest order operator, known as the first-order operator, is given by:

$$\exp\left\{\int_{z}^{z+\Delta z}[L+N(z)]dz'\right\}\cong\exp(\Delta zL)\cdot\exp\left[\int_{z}^{z+\Delta z}N(z')dz'\right]=P_1(\Delta z) \tag{4}$$

As in fact the L and N operators do not commute, this approximation introduces an error of the order $(\Delta z)^2$, as indicated by the Baker-Campbell-Hausdorff (BCH) formula [1], [5]-[9] for non-commutative operators. The operator is then accurate to the first order of Δz, and is said to be of first-order. Smaller errors can be obtained with the higher-order exponential operators.

A second-order operator, largely employed in the literature in conjunction with the SSF method, is obtained by repeated application of the BCH formula, and is given by:

$$\exp\left\{\int_{z}^{z+\Delta z}[L+N(z)]dz'\right\}\cong\exp\left(\frac{\Delta z}{2}L\right)\cdot\exp\left[\int_{z}^{z+\Delta z}N(z')dz'\right]\cdot\exp\left(\frac{\Delta z}{2}L\right)=P_2(\Delta z) \tag{5}$$

The associated error is of the order of $(\Delta z)^3$ [1], [5]-[6].

Higher-order operators are obtained by a symmetric repetition, or product, of the second-order operator given by the equation (5). The 4th- and 6th-order operators are written respectively as [5], [6]:

$$\begin{aligned}&P_4(\Delta z)=P_2(s\Delta z)P_2[(1-2s)\Delta z]P_2(s\Delta z),\ \text{with}\ 2s^3+(1-2s)^3=0\\&P_6(\Delta z)=P_2(s_3\Delta z)P_2(s_2\Delta z)P_2(s_1\Delta z)P_2(s_0\Delta z)P_2(s_1\Delta z)P_2(s_2\Delta z)P_2(s_3\Delta z)\end{aligned} \tag{6}$$

$P_2(\Delta z)$ is given by the equation (5), and s_3 = 0.78451361047756, s_2 = 0.2355733213359357, s_1 = 1.1776799841887, $s_0 = 1 - 2(s_1 + s_2 + s_3)$.

 ISSN 1516-7399

It is easily seen that the operators $P_i(\Delta z)$, i = 2, 4, and 6, require two, six, and fourteen FFTs, respectively, to advance the solution of the equation (2) along one segment Δz. The first-order operator $P_1(\Delta z)$, on the other hand, requires only one FFT.

The error associated with each one of the symmetric exponential operators in the equations (5) and (6) is represented as [5], [6]:

$$\exp\{\Delta z[L + N(z)]\} = P_i(\Delta z) + O\left(\Delta z^{i+1}\right) \quad , \quad i = 2, 4, 6 \tag{7}$$

Higher-order exponential products introduce smaller error, and could allow for longer step size Δz, thus reducing the computing time. However, as the number of required FFTs increases with the order of the operators, the overall error also increases, as shown later on.

The solution of the equation (2) is then approximated as:

$$A(z + \Delta z, T) = P_i(\Delta z) \cdot A(z, T) \quad , \quad i = 1, 2, 4, 6, \ \ldots \tag{8}$$

with the exponential products $P_i(\Delta z)$ being given by the equation (4) for i = 1, and by the equation (5) for i = 2, and by the equation (6) for i = 4, 6.

The equation (8) requires the evaluation of the linear and nonlinear portions of the equation (2), which is done separately in the frequency and time domains, respectively. The linear portion is represented as:

$$\frac{\partial A}{\partial z} = -\frac{j}{2}\beta_2 \frac{\partial^2 A}{\partial T^2} + \frac{1}{6}\beta_3 \frac{\partial^3 A}{\partial T^3} = L \cdot A \tag{9.1}$$

The solution is calculated as [1]:

$$\tilde{A}(z + \Delta z, \omega) = \tilde{A}(z, \omega) \exp\left[\left(\frac{j}{2}\beta_2 \omega^2 + \frac{j}{6}\beta_3 \omega^3\right)\Delta z\right] \tag{9.2}$$

where $\tilde{A}(z,\omega)$ represents the Fourier transform of A(z,T).

The nonlinear portion is represented as:

$$\frac{\partial A}{\partial z} = -\frac{\alpha}{2} A + j\gamma|A|^2 A = N(z) \cdot A \tag{10.1}$$

The solution is calculated as [1]:

$$A(z + \Delta z, T) = \exp\left\{ j\gamma |A(z, T)|^2 \cdot \frac{1 - \exp(-\alpha \Delta z)}{\alpha} - \frac{\alpha}{2}\Delta z \right\} \cdot A(z, T) \tag{10.2}$$

2.2 Multiple Channel Signals

 ISSN 1516-7399

Following the same procedure as indicated in reference [1], the equation (1) is generalised to accommodate the case of multiple frequency signals, or WDM signals. The evolution equation for the optical field at the k^{th} frequency (or the k^{th} WDM channel) is written as [1]:

$$\frac{\partial A_k}{\partial z} + d_k \frac{\partial A_k}{\partial T} + \frac{j}{2}\beta_{2k}\frac{\partial^2 A_k}{\partial T^2} - \frac{1}{6}\beta_{3k}\frac{\partial^3 A_k}{\partial T^3} + \frac{\alpha_k}{2}A_k = j\gamma_k\left(|A_k|^2 + 2\sum_{i\neq k}|A_i|^2\right)A_k \quad (11)$$

where $d_k = \beta_{1k} - \beta_{1ref}$ represents the group velocity mismatch, and $\beta_{1k} = 1/v_{gk}$. β_{1ref} corresponds to the values of β_1 associated to the reference frequency or channel. The parameter β_{1k} depends on the refraction index of the fiber, and its value can be obtained from the dispersion parameter D.

The first and second terms on the right-hand side of the equation (11) represent the effects of self-phase modulation (SPM), and cross-phase modulation (XPM), respectively. The factor 2 indicates that XPM is twice as efficient than SPM, for a given intensity of the optical field. The group velocity mismatch plays an important role, as it determines the interaction between copropagating optical fields. The other parameters in the equation (11) are analogue to those in the equation (1), and in general depend on the wavelength. However, in practice their variation with the wavelength is small and can be neglected.

For the type of optical fiber usually deployed in high-capacity, long distance optical communication systems, a typical profile for the dispersion parameter D is:

$$D(\lambda) = \frac{\delta}{4}\left(\lambda - \frac{\lambda_0^4}{\lambda^3}\right) \quad (12)$$

where $\delta = dD/d\lambda$ is the dispersion slope. The parameters β_1, β_2 e β_3 are defined as:

$$\beta_1 = \int D(\lambda)d\lambda \quad ; \quad \beta_2 = -\frac{\lambda^2}{2\pi c}D(\lambda) \quad ; \quad \beta_3 = -\frac{\lambda^2}{2\pi c}\cdot\frac{d\beta_2}{d\lambda} \quad (13)$$

Using the equation (12), these parameters are easily calculated as:

$$\beta_1 = \frac{\delta}{8}\left(\lambda^2 + \frac{\lambda_0^4}{\lambda^2}\right) \; ; \; \beta_2 = -\frac{\lambda^2}{2\pi c}\cdot\frac{\delta}{4}\left(\lambda - \frac{\lambda_0^4}{\lambda^3}\right) \; ; \; \beta_3 = \frac{\lambda^3}{(2\pi c)^2}\left[2D(\lambda) + \lambda\delta\right] \quad (14)$$

where c is the velocity of light in vacuum. The expressions above must be evaluated for each channel individually. λ_0 is the zero-dispersion wavelength of the optical fiber.

Using the equation (14), the parameter d_k, which represents the group velocity mismatch of the k^{th} channel, is calculated as:

 ISSN 1516-7399

$$d_k = \frac{\delta}{8}\left(\lambda_k^2 - \lambda_{ref}^2\right)\cdot\left(1 - \frac{\lambda_o^4}{\lambda_k^2\lambda_{ref}^2}\right) \qquad (15)$$

where λ_{ref} is a reference wavelength, which can be chosen quite arbitrarily, and can coincide with the wavelength of one of the channels or not.

Once again, for the application of the SSF method, the linear and nonlinear portions of the equation (11) are solved separately. The linear portion is solved in the frequency domain as:

$$\tilde{A}_k(z+\Delta z,\omega_k) = \tilde{A}_k(z,\omega_k)\exp\left[\left(jd_k\omega_k + \frac{j}{2}\beta_{2k}\omega_k^2 + \frac{j}{6}\beta_{3k}\omega_k^3\right)\Delta z\right] \qquad (16)$$

where $\tilde{A}_k(z,\omega)$ represents the Fourier transform of $A_k(z,T)$.

The nonlinear portion of the equation (11) is solved in the time domain as:

$$A_k(z+\Delta z,T) = \exp\left\{j\gamma_k\left(\left|A_k(z,T)\right|^2 + 2\sum_{i\neq k}\left|A_i(z,T)\right|^2\right)\frac{1-\exp(-\alpha\Delta z)}{\alpha} - \frac{\alpha}{2}\Delta z\right\}\cdot A_k(z,T) \qquad (17)$$

3. Results

The formulation of the previous section was implemented in FORTRAN computer programs. The objective of the computer simulation was to evaluate the performance of the exponential operators of the first-, second-, fourth-, and sixth-order. The extensive simulations indicate that in spite of its higher discretization error the first-order operator yielded results comparable to those obtained with the higher-order operators, as it requires only one FFT for each step Δz.

Both standard and dispersion-shifted optical fibers were considered in the simulations. The effective area of fibers was taken as A_{eff} = 50 μm^2, and the value of the third-order susceptibility $\chi^{(3)}$ was set at 4.0x 10^{-15} esu. Throughout the rest of the paper, the step size Δz is obtained from a nonlinear phaseshift $\Delta\phi$, which is an input datum for the simulation. The relation between Δz and $\Delta\phi$ is as follows:

$$\Delta z = \frac{\Delta\phi}{\gamma P_{in}}\exp(2\alpha z) \quad ; \quad \gamma = \frac{3\pi}{4}\cdot\frac{\mathrm{Re}\left(\chi^{(3)}\right)}{n\lambda A_{eff}} \qquad (18)$$

where α is the loss coefficient of the fiber, z represents distance along the length of the fiber, P_{in} is the input peak power, n is the refractive index of the fiber, A_{eff} is its effective area; λ is the operating wavelength, and Re(.) means the real part.

For a lossy fiber, the equation (18) represents a nonuniform spatial discretization, as the step size increases along the length of the fiber.

3.1 Single Channel Signal

Initially, a monochromatic signal was considered. The signal comprised a sequence of two second-order soliton pulses at 1550 nm, and was propagated along a standard optical fiber (zero-dispersion wavelength at 1310 nm). The dispersion slope of the fiber was taken as $\delta = 0.09$ ps/km-nm^2. The transmission rate was set at 2.5 Gbit/s, and 1024 time samples per bit were taken for the FFT. Once the objective of the computer simulation was to evaluate the performance of the exponential operators for nonlinear pulse propagation, the linear loss of the fibers was neglected.

Figure 1 shows the waveform of the second-order soliton pulses after a propagation distance of 500 km, as calculated with the first-, second-, and fourth-order operators. Figure 1-a shows a comparison of the results obtained with the second- and fourth-order operators, using a nonlinear phaseshift $\Delta\phi = 0.005$. In this figure, the solid line traces have been attenuated of 0.2 dB for the sole purpose of helping the visualisation. The agreement between the two results is excellent. However, when the step size was increased (nonlinear phaseshift $\Delta\phi = 0.1$), the result obtained with the fourth-order operator deteriorated considerably, as illustrated by Figure 1-b. A such loss of accuracy is attributed to the greater number of FFTs required by the higher-order operator, as the spatial discretization error associated with it, according to the equation (7), is smaller than the errors associated with the lower-order operators. Figure 1-c shows a comparison of the results obtained with the first- and second-order operators, using a nonlinear phaseshift $\Delta\phi = 0.005$. Although the discretization error of the first-order operator is larger than that of the second-order one, it yields results of the same quality.

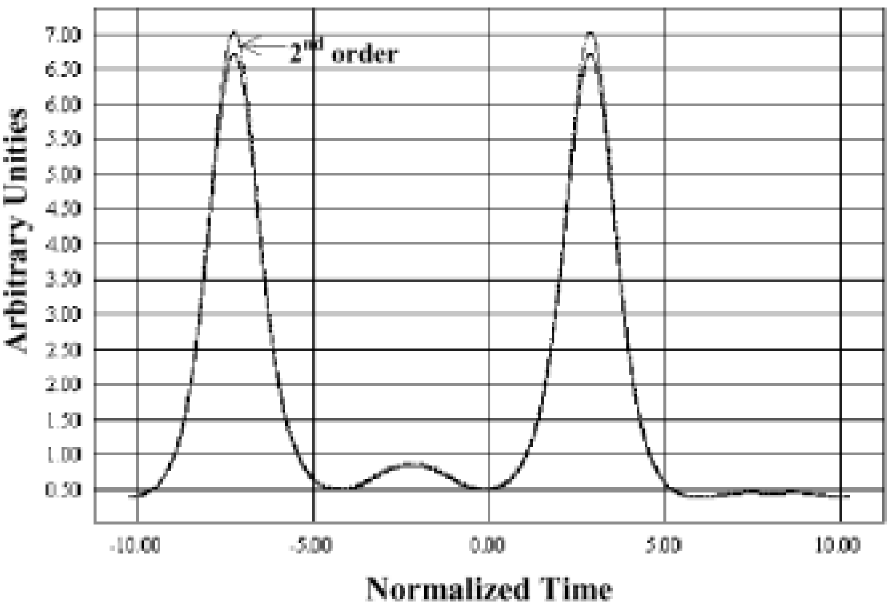

(a)

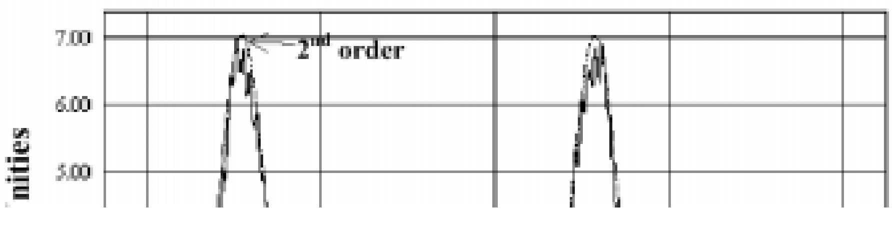

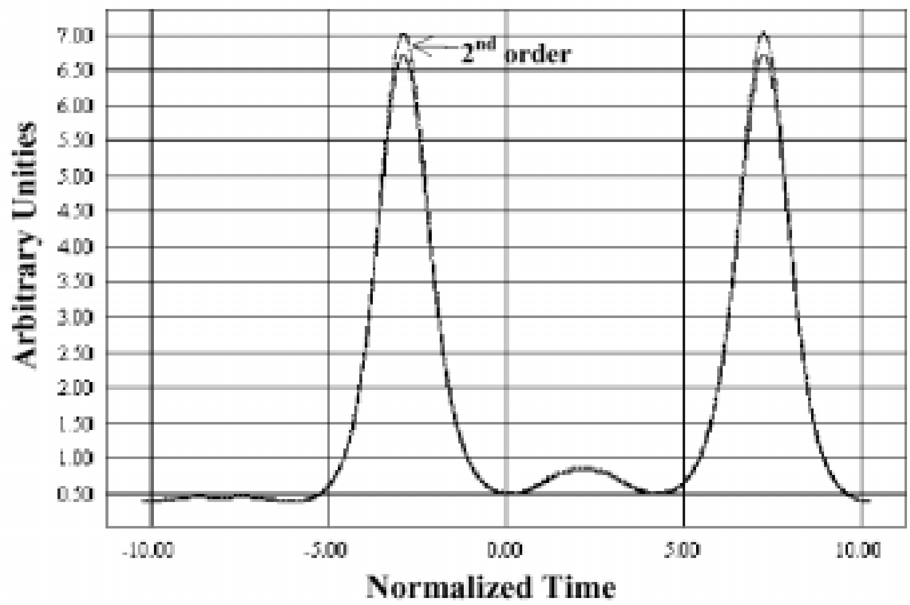

(c)

Figure 1: Waveform of two second-order soliton pulses after 500 km of lossless, standard optical fiber, as calculated with the second- (dashed line) and fourth-order (solid line) exponential operators, with nonlinear phaseshift $\Delta\phi$=0.005 (a), $\Delta\phi$=0.1 (b); first- (solid line) and second- (dashed line) exponential operators, $\Delta\phi$=0.005 (c).

Further simulations showed a rapid deterioration of the results of the fourth-order operator as the step size was increased. Such deterioration was even faster for longer propagation distances and higher input powers, situation that accentuates the nonlinear effects in optical fibers. The same comments apply to the sixth- or even higher-order operators.

3.2 Multiple Channel Signal

 ISSN 1516-7399

A four-channel CW signal was considered next, at the following wavelengths: 1550.25 nm, 1550.75 nm, 1551.25 nm, and 1551.75 nm. The reference wavelenght was taken at 1551 nm, and the input power of each channel was 5 mW. Figure 2 shows the corresponding frequency spectrum as calculated with the second-order operator, using a nonlinear phaseshift $\Delta\phi = 0.005$, and considering 10 km of standard fiber, with a loss coefficient of 0.2 dB/km, and dispersion slope $\delta = 0.09$ ps/km-nm^2. The four carriers and the new frequencies generated by four-wave mixing are clearly seen in this figure.

Figure 3 shows the same frequency spectrum as calculated with the fourth-order operator, and the same step size ($\Delta\phi = 0.005$). The agreement between the two figures is excellent. In Figure 4, the step size was increased ten times ($\Delta\phi = 0.05$), resulting in the appearance of spurious frequency components. Again, the deterioration of the results of the fourth-order operator is credited to the large number of required FFTs.

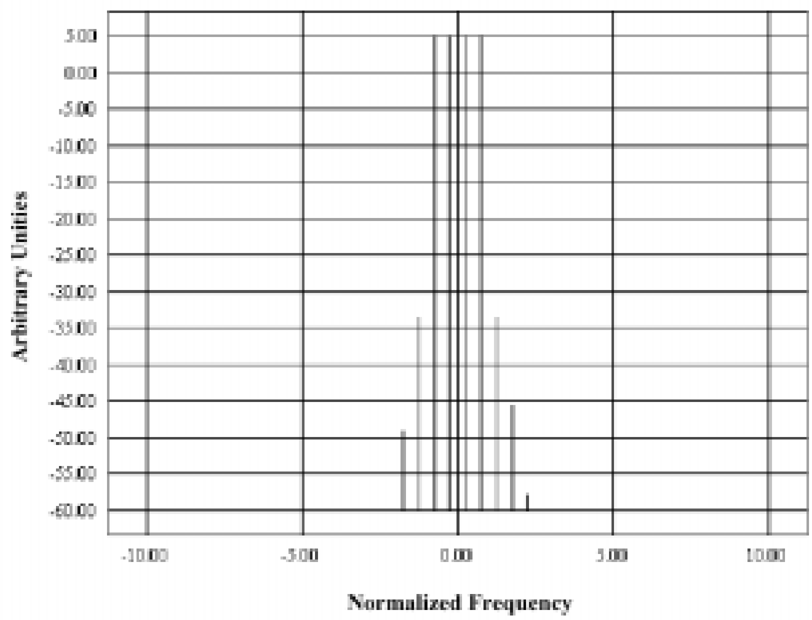

Figure 2: Frequency spectrum of the four-channel signal as calculated with the second-order exponential operator, using a nonlinear phaseshift $\Delta\phi$=0.005.

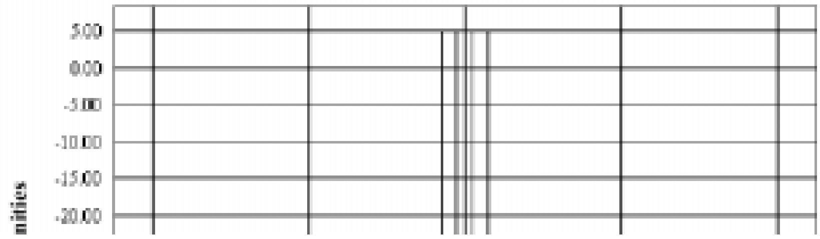

Figure 3: Frequency spectrum of the four-channel signal as calculated with the fourth-order exponential operator, using a nonlinear phaseshift Δϕ=0.005.

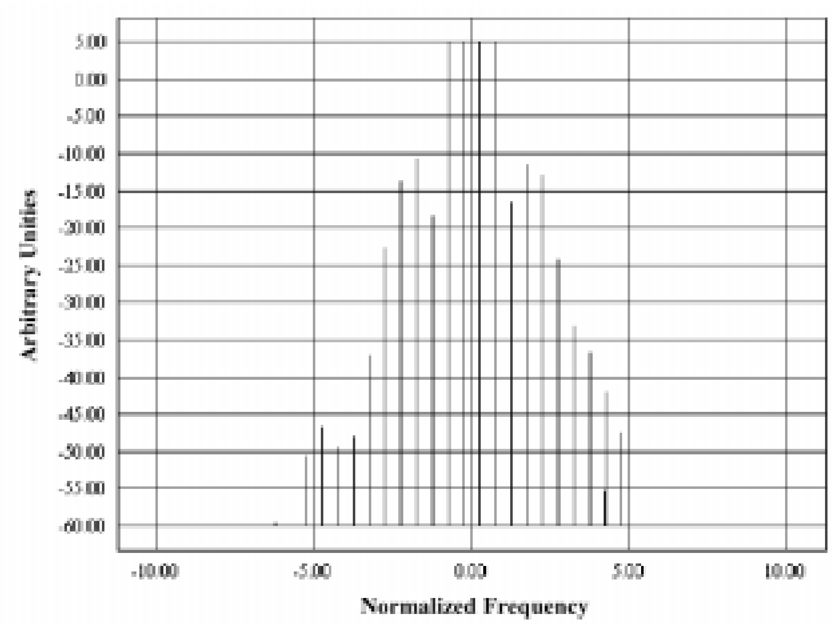

Figure 4: Frequency spectrum of the four-channel signal as calculated with the fourth-order exponential operator, using a nonlinear phaseshift Δϕ=0.05.

Figure 5 shows the same results of Figure 2 as obtained with the first-order model, using a nonlinear phaseshift $\Delta\phi = 0.005$. Although the first-order operator has a larger discretization error, Figure 5 indicates clearly that its results have the same quality as those obtained with higher-order operators (Figures 2 and 3). This fact confirms that the dominant

 ISSN 1516-7399

error in the Split-Step Fourier method is not the one due the spatial discretization, but that accumulated by the successive FFTs.

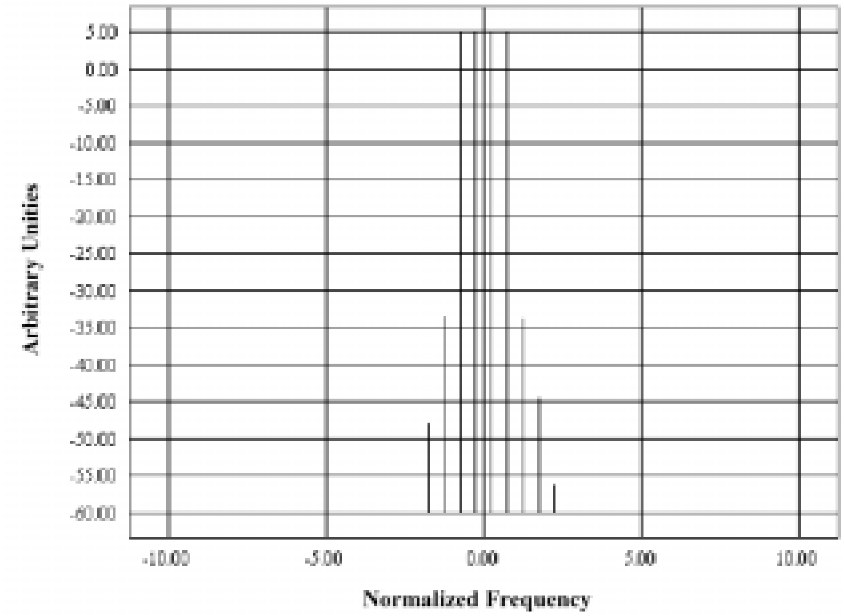

Figure 5: Frequency spectrum of the four-channel signal as calculated with the first-order exponential operator, using a nonlinear phaseshift Δϕ=0.005.

Still considering the same four-channel signal, Figures 6, 7, 8 show the frequency spectrum after 10 km of dispersion-shifted fiber (zero-dispersion wavelength at 1550 nm), loss coefficient of 0.2 dB/km, dispersion slope δ = 0.066 ps/km-nm^2. In Figure 6, the first-order operator was used, with a nonlinear phaseshift Δϕ = 0.005, and the result is in perfect agreement with theory [1]. In Figure 7, the second-order operator was used, also with Δϕ = 0.005. Once more, the first-order operator yielded results of the same quality as those obtained with higher-order operators, for the same step-size.

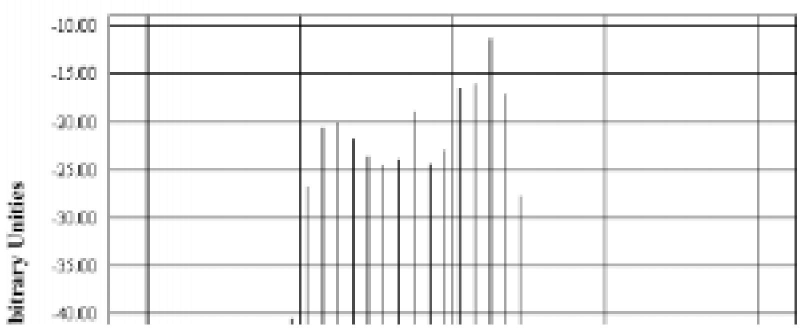

 SN 1516-7399

Figure 6: Frequency spectrum of the four-channel signal as calculated with the first-order exponential operator, using a nonlinear phaseshift Δϕ=0.005 (after 10 km of dispersion-shifted fiber).

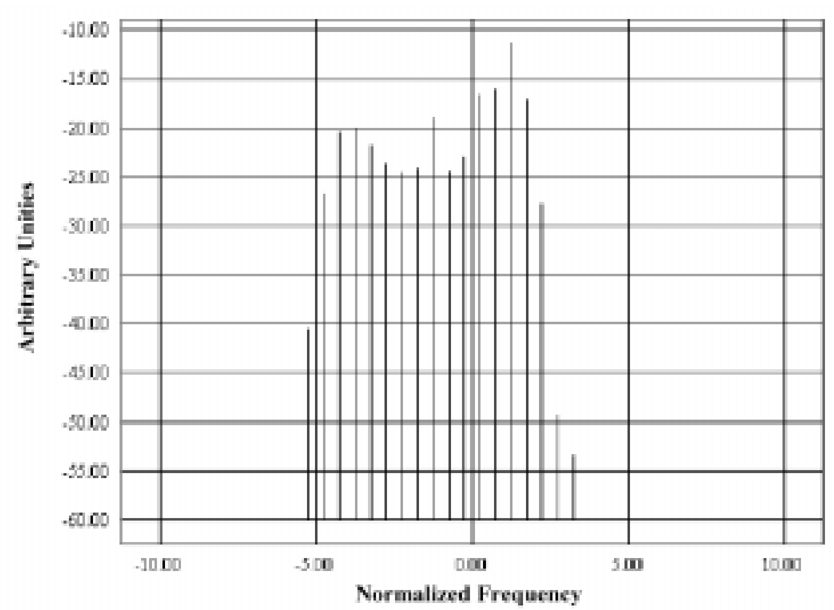

Figure 7: Frequency spectrum of the four-channel signal as calculated with the second-order exponential operator, using a nonlinear phaseshift Δϕ=0.005 (after 10 km of dispersion-shifted fiber).

 ISSN 1516-7399

In Figure 8, the fourth-order operator was used with a much larger step-size ($\Delta\phi = 0.01$), and spurious frequency components appeared again.

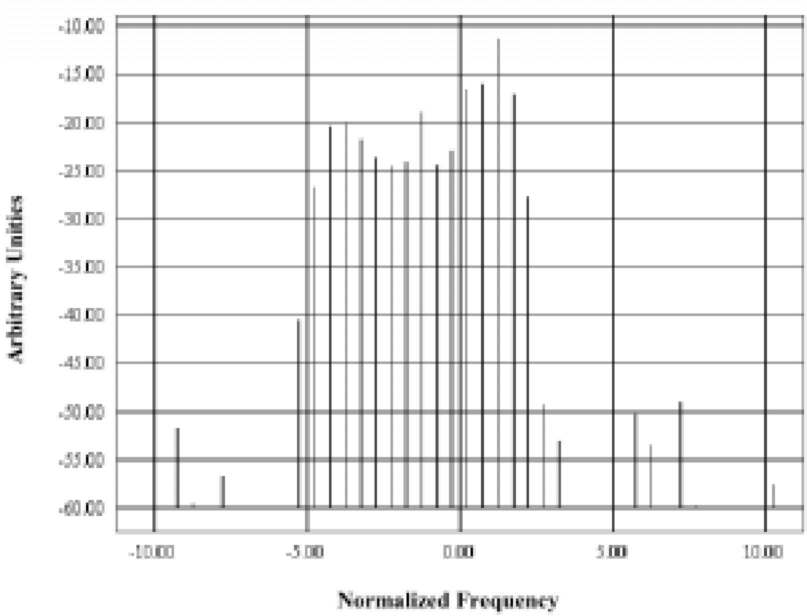

Figure 8: Frequency spectrum of the four-channel signal as calculated with the fourth-order exponential operator, using a nonlinear phaseshift $\Delta\phi=0.01$ (after 10 km of dispersion-shifted fiber).

4. Conclusion

This paper presented an assessment of exponential operators of different orders used in the numerical integration of the generalised nonlinear Schrödinger, with applications in optical communication systems, by means of the Split-Step Fourier Method. Exponential operators of the first-, second-, fourth-, and sixth-orders were considered for an approximate solution of the equation (3). Two sources of errors were identified: the spatial discretization and the FFT. It was observed that although the higher-order exponential operators introduced smaller discretization error, the total error in the application of the SSF method is dominated by the error introduced by the FFT.

Numerous simulations were carried out using FORTRAN computer programs. In the case of single channel systems, the results indicate that the simpler first-order exponential operator is superior that the higher-order ones, for a given step size. The poorer performance of the higher-order operators is attributed to the larger number of FFTs they require, as compared with the first-order one. The deterioration of the results obtained with the fourth- and higher-order operators is even more significant for longer propagation distances and/or higher input powers, situations that accentuate the nonlinear effects in optical fibers.

For WDM systems, the problem is more complex, mainly due to the four-wave mixing process, which generates new frequency components, and so limits the capacity of the system. Considering a four-channel system, it was observed that the step size must be kept

 ISSN 1516-7399

sufficiently small to avoid the introduction of spurious frequency components, independent of the order of the exponential operator used. The rapid deterioration of the results obtained with the fourth- and higher-order operators makes their application not viable.

It is worth mentioning that many papers on higher-order exponential operators, or symplectic integrators can be found in the literature, e.g. [6]-[9], focusing on the reduction of the discretization error. When these operators are used in conjunction of the SSF method, the simulations carried in the present work showed that the error introduced by the FFT is dominant, and cancels any benefit provided by the higher-order operators. On the whole, the first-order operator yielded the best results, considering both the accuracy and computing time: the first-order operator allowed for a reduction of 10% to 20% of the computing time, depending on the complexity of the problem, in comparison with the second-order operator, which was taken as a reference, once it is largely employed in the literature in conjunction with the SSF method.

References

[1] G. P. Agrawal: "*Nonlinear Fiber Optics*", Academic Press, 2nd Edition, 1995.

[2] T. R. Taha, and M. J. Ablowitz: "Analytical and numerical aspects of certain nonlinear evolution equations. II. Numerical, nonlinear Schrödinger equation", J. Comp. Phys., Vol. 55, pp.203-230, 1984.

[3] J. A. C. Weideman, and B. M. Herbst: "Split-step methods for the solution of the nonlinear Schrödinger equation", SIAM J. Numer. Anal., Vol. 23, pp. 485-507, 1986.

[4] H. Ghafouri - Shiraz, P. Shum, and M. Nagata: "A novel method for analysis of soliton propagation in optical fibers", IEEE J. Quantum Electron. Vol. 31, pp. 190-200, 1995.

[5] T. Gornsztejn, and J. R. Souza: "Numerical Schemes for Optical Soliton Propagation Analysis: A Test Comparison", Proceedings of the 1997 SBMO/IEEE MTT-S International Microwave and Optoelectronics Conference, pp. 543-547, 1997.

[6] D. Bandrauk, and H. Shen: "High-order split-step exponential methods for solving coupled nonlinear Schrödinger equations", J. Phys. A: Math. Gen., Vol. 27, pp. 7147-7155, 1994.

[7] H. Yoshida: "Construction of higher order symplectic integrators", Phys. Lett. A, Vol. 150, pp. 262-268, 1990.

[8] J.E.Chambers, and M.A.Murison: "Pseudo-High-Order Symplectic Integrators", http://arnold.usno.navy.mil/murison/Papers/Symplectic/paper1.pdf.

[9] G. Dattoli, L. Giannessi, M. Quattromini, and P. L. Ottaviani: "Symmetric decomposition of exponential operators and evolution problems", Pys. Lett. A, Vol. 247, pp 191-197, 1998.

 ISSN 1516-7399